NASA/TP-2006-213950

A Compact Efficient Lidar Receiver for Measuring Atmospheric Aerosols

Christopher Gili
Old Dominion University, Norfolk, Virginia

Russell De Young
Langley Research Center, Hampton, Virginia

January 2006

The NASA STI Program Office . . . in Profile

Since its founding, NASA has been dedicated to the advancement of aeronautics and space science. The NASA Scientific and Technical Information (STI) Program Office plays a key part in helping NASA maintain this important role.

The NASA STI Program Office is operated by Langley Research Center, the lead center for NASA's scientific and technical information. The NASA STI Program Office provides access to the NASA STI Database, the largest collection of aeronautical and space science STI in the world. The Program Office is also NASA's institutional mechanism for disseminating the results of its research and development activities. These results are published by NASA in the NASA STI Report Series, which includes the following report types:

- TECHNICAL PUBLICATION. Reports of completed research or a major significant phase of research that present the results of NASA programs and include extensive data or theoretical analysis. Includes compilations of significant scientific and technical data and information deemed to be of continuing reference value. NASA counterpart of peer-reviewed formal professional papers, but having less stringent limitations on manuscript length and extent of graphic presentations.

- TECHNICAL MEMORANDUM. Scientific and technical findings that are preliminary or of specialized interest, e.g., quick release reports, working papers, and bibliographies that contain minimal annotation. Does not contain extensive analysis.

- CONTRACTOR REPORT. Scientific and technical findings by NASA-sponsored contractors and grantees.

- CONFERENCE PUBLICATION. Collected papers from scientific and technical conferences, symposia, seminars, or other meetings sponsored or co-sponsored by NASA.

- SPECIAL PUBLICATION. Scientific, technical, or historical information from NASA programs, projects, and missions, often concerned with subjects having substantial public interest.

- TECHNICAL TRANSLATION. English-language translations of foreign scientific and technical material pertinent to NASA's mission.

Specialized services that complement the STI Program Office's diverse offerings include creating custom thesauri, building customized databases, organizing and publishing research results ... even providing videos.

For more information about the NASA STI Program Office, see the following:

- Access the NASA STI Program Home Page at ***http://www.sti.nasa.gov***

- E-mail your question via the Internet to help@sti.nasa.gov

- Fax your question to the NASA STI Help Desk at (301) 621-0134

- Phone the NASA STI Help Desk at (301) 621-0390

- Write to:
  NASA STI Help Desk
  NASA Center for AeroSpace Information
  7121 Standard Drive
  Hanover, MD 21076-1320

NASA/TP-2006-213950

A Compact Efficient Lidar Receiver for Measuring Atmospheric Aerosols

Christopher Gili
Old Dominion University, Norfolk, Virginia

Russell De Young
Langley Research Center, Hampton, Virginia

National Aeronautics and
Space Administration

Langley Research Center
Hampton, Virginia 23681-2199

January 2006

Available from:

NASA Center for AeroSpace Information (CASI)
7121 Standard Drive
Hanover, MD 21076-1320
(301) 621-0390

National Technical Information Service (NTIS)
5285 Port Royal Road
Springfield, VA 22161-2171
(703) 605-6000

ABSTRACT

A small, light weight, and efficient aerosol lidar receiver was constructed and tested. Weight and space savings were realized by using rigid optic tubes and mounting cubes to package the steering optics and detectors in a compact assembly. The receiver had a 1064nm channel using an APD detector. The 532nm channel was split (90/10) into an analog channel (90%) and a photon counting channel (10%). The efficiency of the 1064nm channel with optical filter was 44.0%. The efficiency of the analog 532nm channel was 61.4% with the optical filter, and the efficiency of the 532nm photon counting channel was 7.6% with the optical filter.

The results of the atmospheric tests show that the detectors were able to consistently return accurate results. The lidar receiver was able to detect distinct cloud layers, and the lidar returns also agreed across the different detectors. The use of a light weight fiber-coupled telescope reduced weight and allowed great latitude in detector assembly positioning due to the flexibility enabled by the use of fiber optics. The receiver is now ready to be deployed for aircraft or ground based aerosol lidar measurements.

1.0 INTRODUCTION

In the past few decades, the issues related to anthropogenic global warming have caused great concern within the scientific community, as well as the general public. One particular area of great interest is the effect of aerosols on climate and global warming. At present, there are a number of different instruments on ground-based, airborne, and satellite platforms, all designed to measure and track the influence of aerosols on climate change.

Aerosols play an important role in climate, and behave in a manner similar to clouds, reflecting energy back into space thus cooling the atmosphere (1,2). Carbon aerosols can absorb sunlight, and thus they can heat the atmosphere. Aerosols play an indirect role as well, as they can act as condensation nuclei for cloud formation. The size and shapes of the aerosol particles are also a factor here, as they influence the properties of the clouds they help form. Smaller aerosol particles can inhibit rainfall, because the water droplets that collect around them are smaller, so they take longer to condense into enough mass to fall as rain. The types and sources of aerosols in the atmosphere vary greatly. There are natural sources: pollen from plants, salt from sea spray, dust from sand storms, and ash from volcanic eruptions. There are also man-made sources: ash, soot, and chemicals from industrial smokestacks and automobiles, fires from slash-and-burn deforestation, dust from wind erosion. The altitude of these aerosols is important, because particles at lower altitudes are likely to be washed out of the atmosphere by rain, and will not have a long term effect on the climate. But those that achieve a higher altitude are likely to remain airborne much longer, and will travel greater distances, influencing global climate patterns far from the point of origin.

Air pollution is a growing health concern as well, and aerosols can have an adverse effect on air quality and population health. The concerns are myriad: aerosols are believed to contribute to pulmonary and cardiovascular complications; some chemicals are toxic, others are believed to be carcinogens. Due to the small size of

aerosols, they can easily be inhaled and penetrate deep into the lungs, where they can accumulate and have the potential to cause problems similar to asbestos-related lung cancer or black lung disease caused by coal dust.

Aerosol lidar systems are now being used routinely around the world to monitor aerosol concentrations near population centers. The basic lidar configuration consists of a laser transmitter, a receiver assembly, and data processing equipment. A pulse of light is emitted from the laser, and as the beam travels through the atmosphere, it encounters particles (molecules, aerosols, water droplets, etc.) that scatter the light and reflect some of it back towards the ground. A telescope aimed at the same atmospheric volume as the laser pulse will capture the backscattered photons and send them to an optical receiver (4). Since light travels at $3x10^8$ m/sec, the aerosol or cloud distance or range can be calculated as range = 0.5tc where c is the speed of light and t is the time the cloud signal return was recorded at the receiver (3).

Our goal was to design a highly compact, efficient lidar detection receiver system, using a fiber coupled telescope, that would be integrated into an existing airborne aerosol lidar system in order to provide a lower mass and volume alternative for obtaining measurements of aerosol distributions.

2.0 LIDAR HARDWARE DESCRIPTION

An existing aerosol lidar at NASA Langley Research Center has been used to measure aerosols both from aircraft and ground locations (5). For aircraft deployment, weight and size are important considerations and should be reduced as much as possible. With this in mind, a design study was initiated to replace the current lidar receiver with a lighter, more compact efficient design. The results of this investigation are reported here.

2.1 OPTICS AND DETECTORS

The lidar system used a Nd:YAG (Big Sky CRF-200) pulsed 20 Hz laser that emits at 1064 nm and also uses a frequency doubler to also provide 532 nm pulses. The backscattered laser returns are captured by a telescope, consisting of a custom Stabilite Cellular 30.5cm diameter f/2 parabolic mirror mounted in a carbon epoxy tube. A bracket was fabricated to mount the end of a 1mm diameter SMA optical fiber (Ceram-Optec UV1000) at the focal point of the telescope mirror as shown in figure 1. The output from the fiber optic is passed to the receiver box. Here the beam is expanded and collimated (Thor Labs F810SMA), as shown in figure 2. Then the light is sent through a beam splitter (HR @ 532nm, HT @ 1064nm) which splits the beam into two channels, one at 1064nm and the other at 532nm. Each channel has a narrowband optical filter to isolate the desired wavelengths and reduce the background light level: 66.5%T 10nm FWHM 532nm filter and a 78.0%T 1nm FWHM 1064nm filter were used.

The 1064nm beam passes through the filter and then is focused by an aspheric lens (30mm f.l.) onto a Perkin-Elmer 30955E avalanche photodiode (APD) detector. An APD was chosen for the 1064nm detector because photomultiplier tubes have low quantum efficiency at 1μm wavelengths. The APD is powered by a high voltage power supply (EMCO CA05P), and the output signal is amplified by an amplifier (Femto

DHPVA-100) then sampled at 5MHz by a 14-bit digitizer (Gage Applied Sciences 1450), as shown in figure 3.

The 532nm beam is reflected off the first beam splitter, passes through the 532nm filter, and is split again. One 532nm beam passes through (90%) the beam splitter and is focused by an aspheric lens (28mm f.l.) onto an analog photomultiplier (PMT) tube (Perkin-Elmer MH-943). The second 532nm beam is reflected (10%) off the beam splitter and is focused by an aspheric lens (28mm f.l.) onto a photon counting tube (Perkin-Elmer MP-943). A photomultiplier tube was used because they have good quantum efficiency at 532nm and have a large linear range of operation. The photon counter was selected because it is very sensitive detecting single photon returns, below the threshold of the analog PMT. Both detectors are powered by a 5V power supply. The analog PMT is sampled by the same Gage digitizer used with the APD. The PC detector sends pulses to a multichannel scalar card (Perkin-Elmer Pci-MCS), where the lidar return signal built up over some integration time. The sample bin was 100ns, and typical integration time was 20-30 seconds. Both the digitizer and multichannel scalar cards are managed using a standard Intel Pentium 4 (2.66GHz) personal computer running Microsoft Windows 2000. The sampled data is recorded by a custom application from within National Intruments' LabVIEW program. The PC detector data is captured by custom software provided by Perkin Elmer.

2.2 MOUNTING HARDWARE

To achieve a compact yet rigid receiver design, we selected the 50.8mm tubes and 80 mm cube optic mount hardware (Thor Labs), as shown in figure 3. The input into the system is a SMA-connected 0.94" optical collimator. The collimator assembly (F810SMA) is mounted on a 60mm cube that houses the 532nm/1064nm beam splitter. A tube is mounted to the cube face opposite the input, and contains the 1064nm filter and a focus lens. A custom plate was fabricated to mount the APD to the end of the tube, using threaded rods and an XY translation mount to locate the active area (1.5mm diameter) of the APD at the focal point of the lens. The 532nm filter is mounted in a tube adjacent (clockwise from above) to the cube face housing the input. Another 60mm cube housing the 532nm beam splitter is attached to the end of this tube. Adjacent (clockwise from above) to the 532nm filter is a tube housing a focus lens, with the PC detector mounted on a custom plate. On the opposite face of the cube is another tube with a focus lens, and then a mounting plate for the analog PMT. This configuration is compact measuring 307mm by 278mm by 82mm, weighing 6 lbs. and structurally rigid, allowing precise alignment of the optical pathways. A photo of the fiber coupled telescope and the optical receiver is shown in Fig. 4.

3.0 EFFICIENCY RESULTS

An experiment was set up to measure the optical efficiency of the receiver. A 6mW CW Nd:YAG laser (Shanghai Uniwave Technology Company DPGL-3005) emitted a beam at both 532 and 1064nm. These beams were separated by a prism into two separate beams and then sent individually into the receiver input. An optical power meter (Newport 840-C) was used to measure the optical power at the receiver input and

at each of the detectors. The 532nm beam was measured to be 3.768mW at the receiver input, and resulted in 2.965mW (78.7% efficient) at the analog PMT and 0.371mW (9.7%) at the PC detector, close to the 90/10% ideal beam splitter expected values. This efficiency was measured without the 532nm filter (78%T) in place, which would drop the efficiencies to 61.4% at the analog PMT detector and 7.6% at the PC detector. The 1064nm beam was measured to be 1.28mW at the receiver input, and gave 0.563mW at the APD, or 44.0% efficient, which is the total efficiency including the 66.5%T 1064nm filter. Some optical losses are due to the collimator assembly, as those lenses are anti-reflection coated for the 420nm to 650nm wavelength region, and not 1064nm.

4.0 ATMOSPHERIC LIDAR RESULTS

Atmospheric lidar tests, from NASA Langley Research Center, were conducted on November 10, 2005, for 12 minutes. Skies were clear to slightly foggy when lidar data began, and soon after a distinct cloud layer (low and thin, with intermittent gaps) became visible at about 2.5km altitude as shown in figures 5, 6 and 7. In these figures, the lidar return signal (2-sec. profiles) has been background subtracted then range squared. The resulting relative signal intensity is plotted in the right panel on a color scale. Large backscattered signals such as clouds can easily be seen in the panel as a function of time. The left panel is a single 2-second lidar profile (30-m vertical resolution) taken at the red line in the right panel. In this panel the telescope field-of-view and the laser beam fully overlap at about 200m, and then the lidar return from the atmospheric molecular density is seen. At 2.5km a large backscatter signal is seen, indicating a cloud at the top of the boundary layer. In the right panel, after about 90 seconds of lidar data, a cloud layer moves into the lidar field-of-view, and is visible at an altitude of about 2.5km in figures 4 and 5. The APD is less sensitive than the analog 532nm detector, so signal levels in figure 5 are lower than levels in figure 6. In figure 6 the cloud is opaque to the 532nm laser, thus only noise is seen above the cloud.

The photon counting data was taken using a 20 second integration time with a vertical resolution of 15 m. Thirty six lidar returns (20-seconds each) were captured for a total data time of 36 x 20 seconds or 12 minutes as shown in figure 7. The right panel shows the lidar return on a color scale, and in the left panel a single 20 second profile is shown corresponding to the red line in the right panel. The data agree with the analog lidar data of figure 6; at the beginning of the data run, the boundary layer had a diffuse fog, but when the cloud formed the boundary layer cleared and only a cloud return is visible at the top of the boundary layer.

In figure 8, 9, and 10, individual lidar files (each background subtracted and then range squared) from each detector are compared to the 1976 U.S. Standard Atmospheric Density. As the lidar beam starts to overlap the field-of-view of the receiver telescope, the signal of each detector increases until there is complete overlap. At this point, the range squared lidar return follows the standard atmospheric density until the signal is lost in the noise. A cloud return is seen at 2.5km in figures 8 and 9, but for the photon counting return of figure 10 only clear atmosphere was sampled. The 1064nm APD detector is much less sensitive than the 532nm detector, since the altitude at which the 1064nm return follows the atmospheric density is limited compared to the 532 detector.

We also compared the 532nm PMT return to the 1064nm APD return, as seen in figure 11, and to the 532nm PC return, as seen in figure 12. The PMT return and APD return both show strong peaks at identical altitudes of 2.5km and 3km, corresponding to the presence of clouds. The PMT and APD detectors were sampled by the same digitizer and at the same rate, so the files compared were captured at the exact same time. When comparing the 532nm PMT and the 532nm PC returns, the photon counting return is missing a strong signal at 3km. This is because the PMT and PC detectors were sampled at different rates (two seconds compared to 20 seconds), and so the PMT and PC comparisons are from different sampling times.

The receiver operated as expected giving reliable lidar returns from both the atmospheric molecules and clouds. It will now be incorporated into the airborne aerosol lidar system.

5.0 CONCLUSIONS

A small, light weight, and efficient aerosol lidar receiver was constructed and tested. Weight and space savings were realized by using rigid optic tubes and mounting cubes to package the steering optics and detectors in a compact assembly. The receiver had a 1064nm channel using an APD detector. The 532nm channel was split (90/10) into an analog channel (90%) and a photon counting channel (10%). The efficiency of the 1064nm channel with optical filter was 44.0%. The efficiency of the analog 532nm channel was 61.4% with the optical filter, and the efficiency of the 532nm photon counting channel was 7.6% with the optical filter.

The results of the atmospheric tests show that the detectors were able to consistently return accurate results. The lidar receiver was able to detect distinct cloud layers, and the lidar returns also agreed across the different detectors. The use of a light weight fiber-coupled telescope reduced weight and allowed great latitude in detector assembly positioning due to the flexibility enabled by the use of fiber optics. The receiver is now ready to be deployed for aircraft or ground based aerosol lidar measurements.

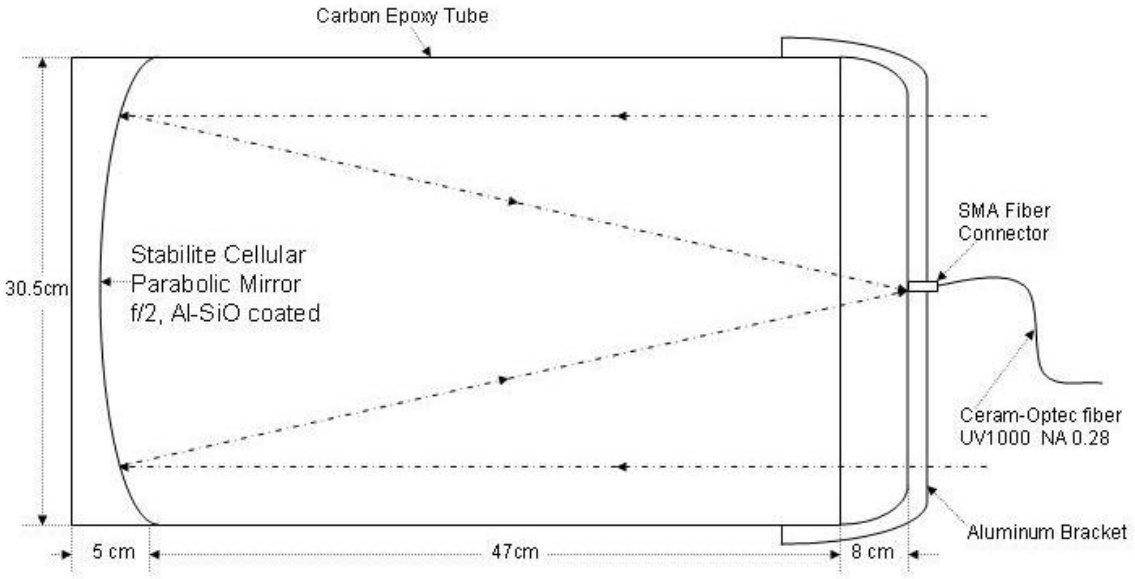

Fig. 1 Fiber-coupled telescope.

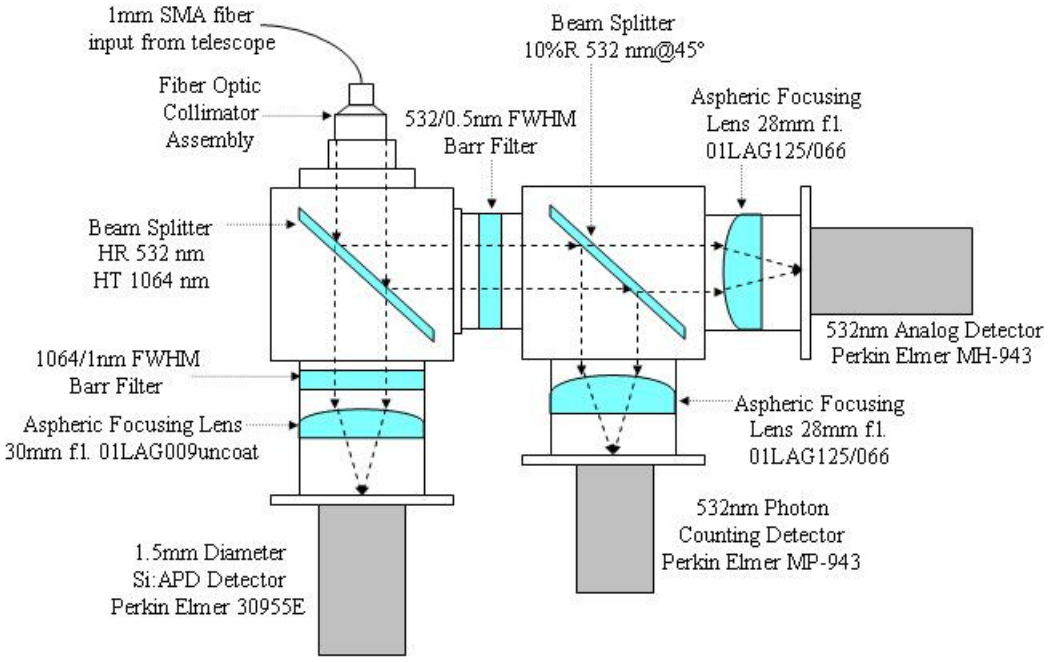

Fig. 2 Layout of optics within rigid mounting structure.

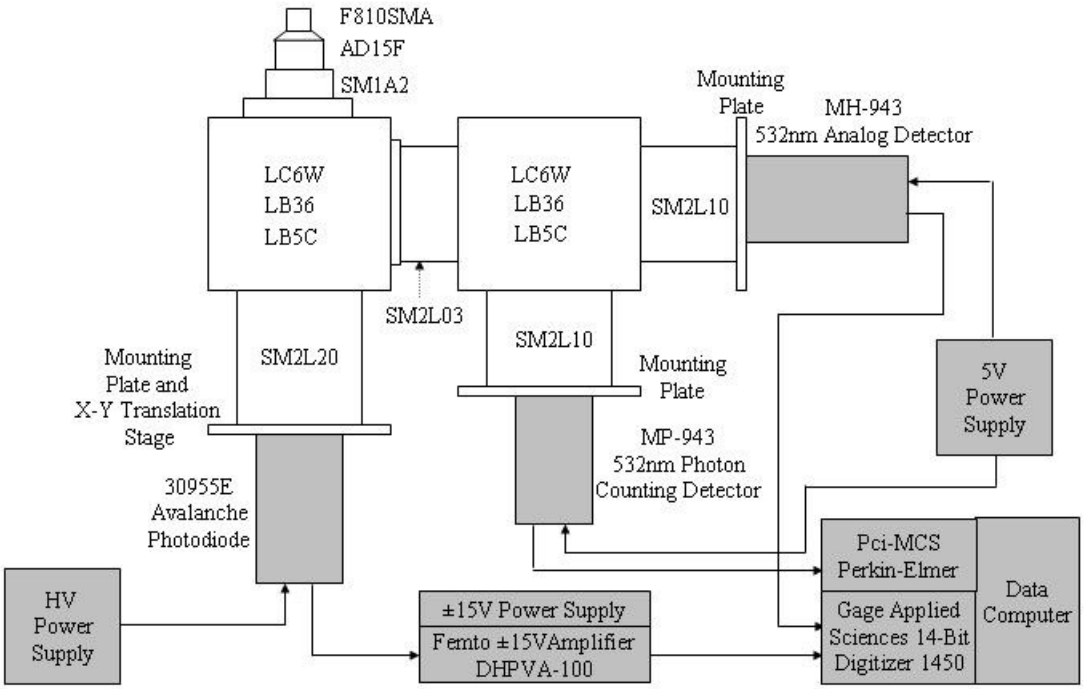

Fig. 3 Layout of optics mounting system and detector electrical components.

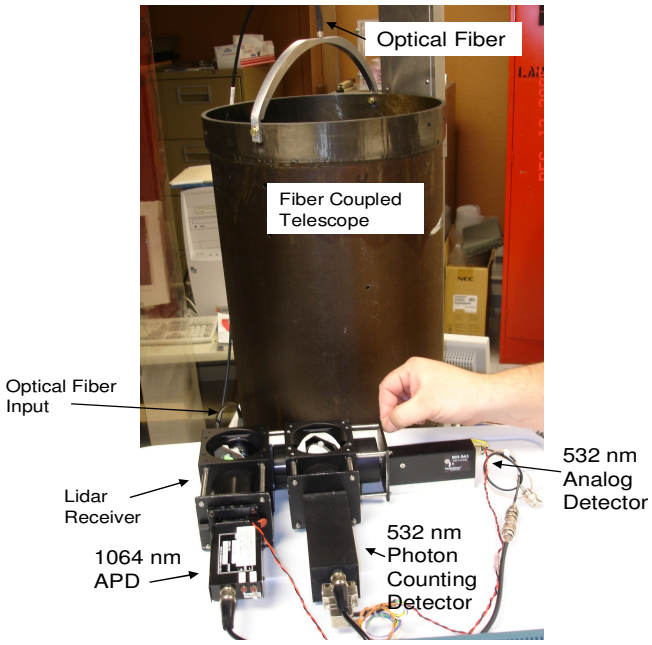

Fig. 4 Photo of fiber coupled telescope and lidar receiver.

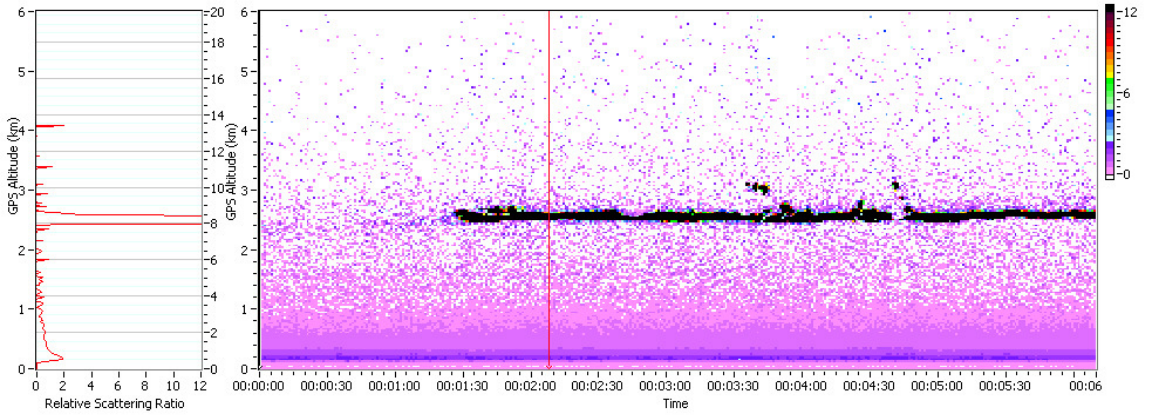

Fig. 5 1064nm lidar return detected by the avalanche photodiode. The total time was 12 minutes. The color panel shows the intensity of the back scattered signal in a color scale (0-12). A thin cloud is seen at about 2.5km. The left panel shows an individual 2-second profile located at the red line in the right panel. The signal has been background subtracted and range squared.

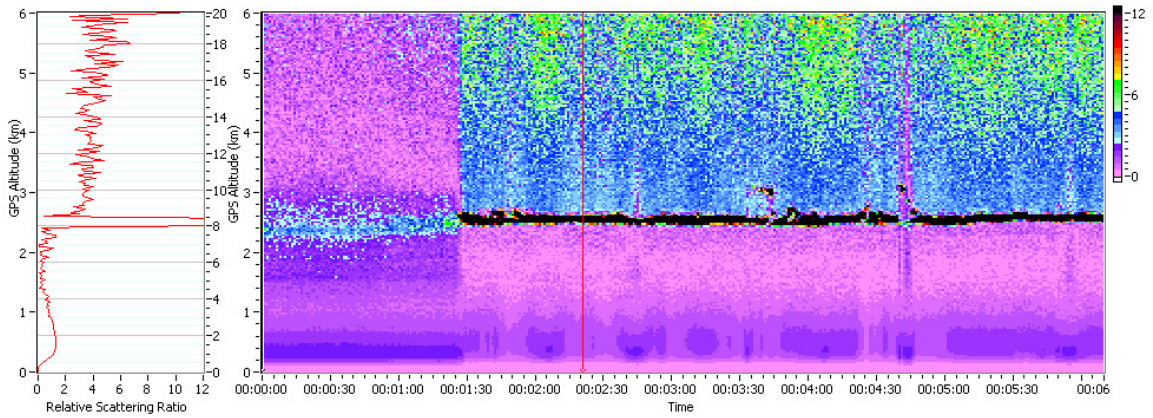

Fig. 6 532nm lidar return detected by the analog photomultiplier tube. The right panel shows the lidar backscatter signal on a color scale (0-12). A thin cloud is seen at about 2.5km as shown in fig. 4. The right panel is a 2-second profile taken at the red line of the right panel. The signal has been background subtracted and range squared.

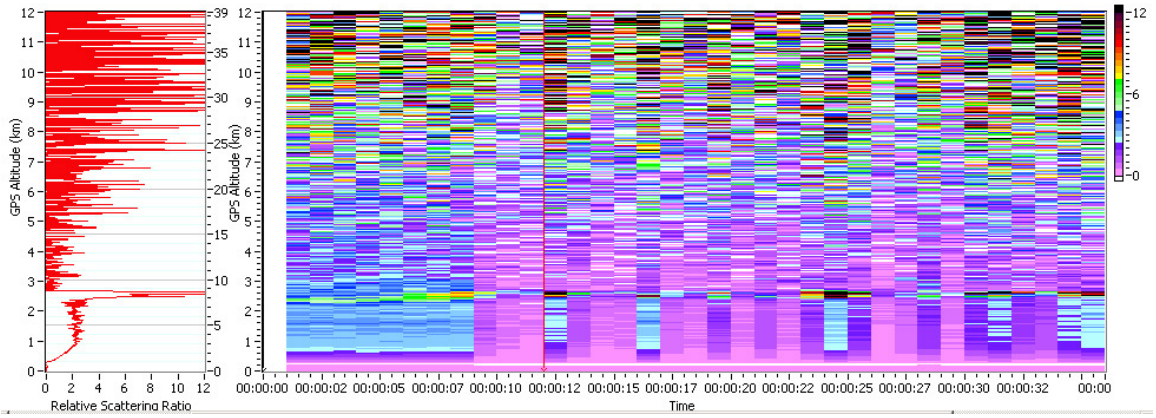

Fig. 7 532nm lidar return detected by the photon counter channel. The signal is plotted using a color scale (0-12) in the right panel. Again a thin cloud layer is seen at 2.5km as shown in fig. 5. The left panel is a 20-second profile taken at the red line in the right panel. The signal has been background subtracted and range squared. With 15-meter vertical resolution, more of the cloud structure can be seen.

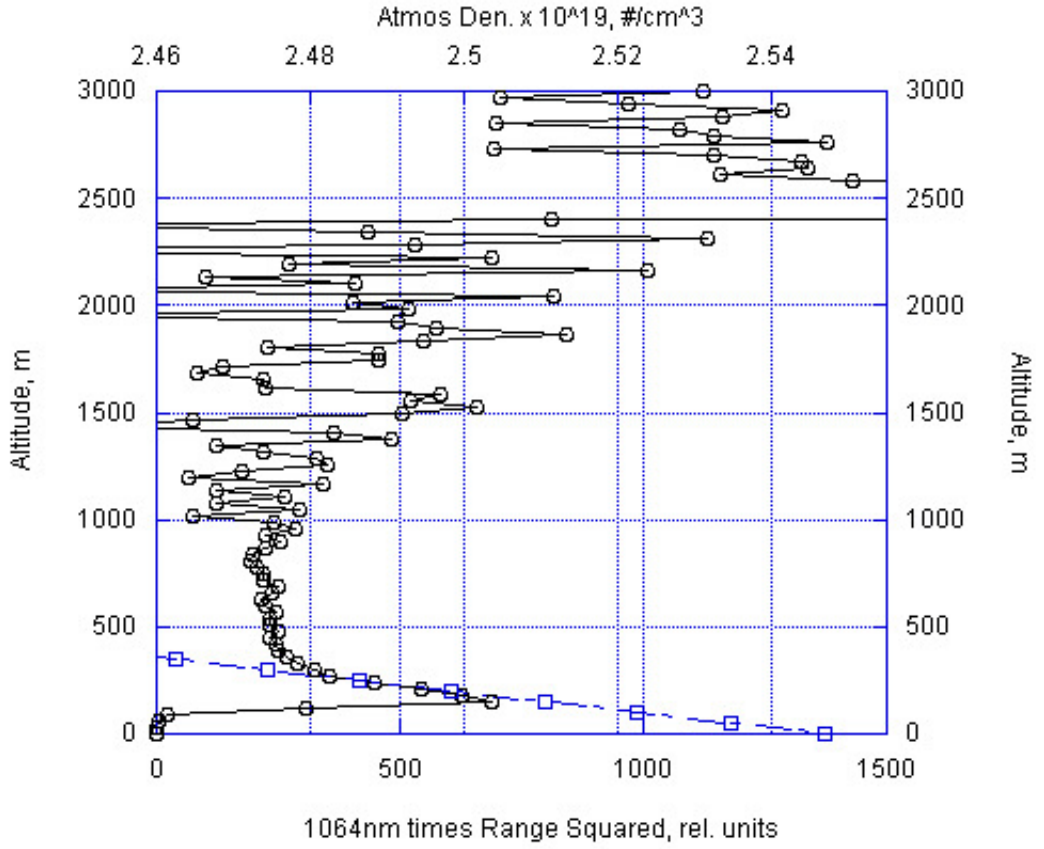

Fig. 8 1064nm APD lidar return (two-second) vs. standard atmospheric density. The atmospheric density has been scaled to match the lidar return. A strong cloud return is seen at about 2.5km. Vertical resolution is 30 meters.

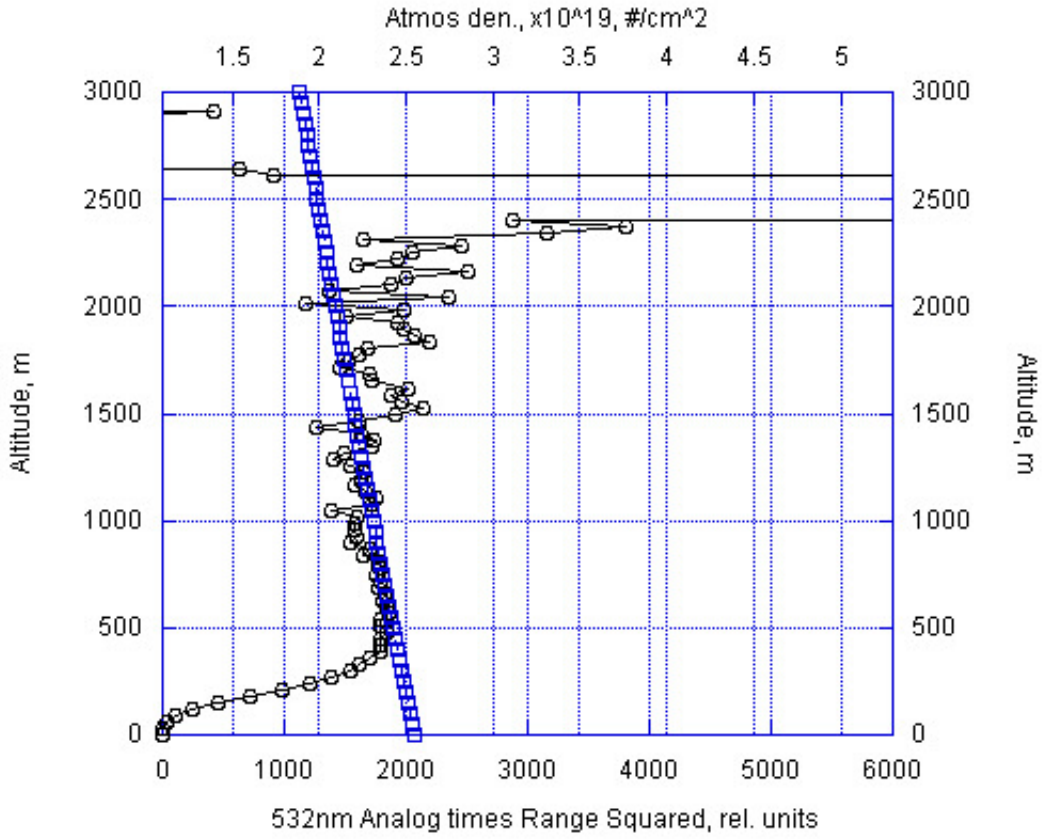

Fig. 9 532nm PMT lidar return (two-second) vs. standard atmospheric density. The atmospheric density has been scaled to match the lidar return. A strong cloud return is seen at about 2.5km. Vertical resolution is 30 meters.

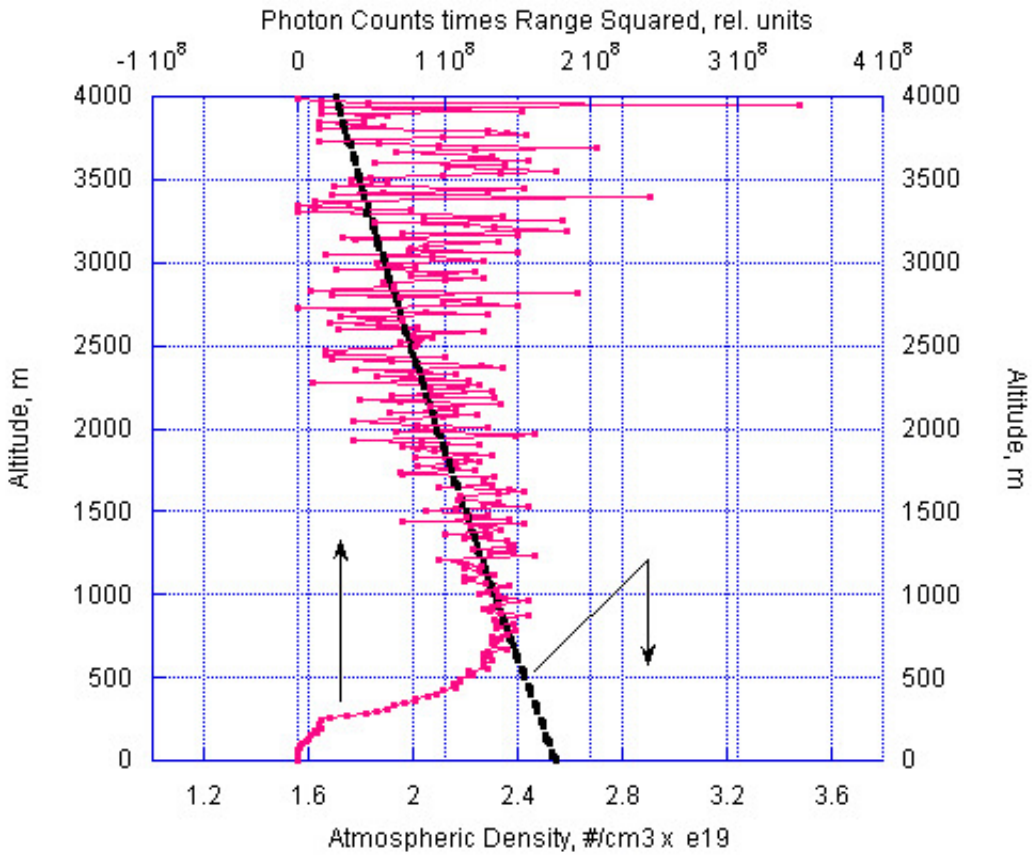

Fig. 10 532nm photon counting lidar return (20-second) vs. standard atmospheric density. The atmospheric density has been scaled to match the lidar return. This profile was taken in clear (no cloud) atmospheric conditions. Vertical resolution is 15 meters.

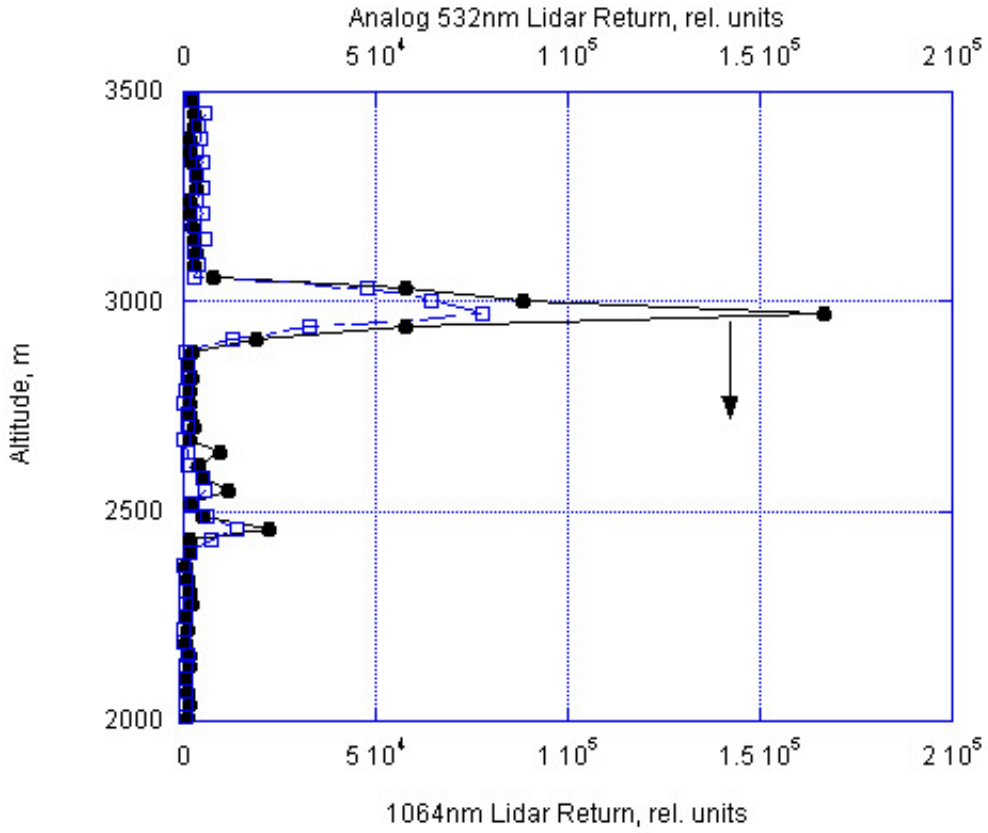

Fig. 11 1064nm APD lidar return compared to analog 532nm lidar return. Both have been background subtracted and range squared.

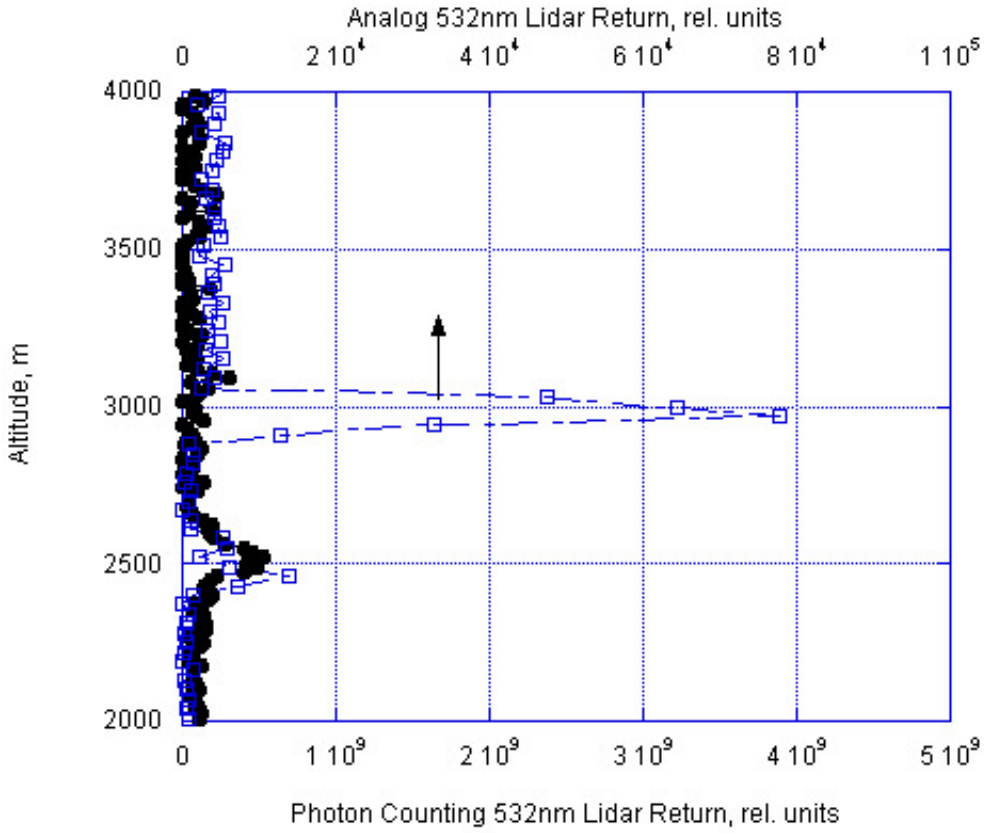

Fig. 12 Analog 532nm lidar return compared to 532nm photon counting lidar return. Both have been background subtracted and range squared.

6.0 REFERENCES

1. Lohmann, U., Wild, M., Solar Dimming, Global Change Newsletter, No. 63, pp. 21-23, Sept. 2005.

2. Graedel, T.E.; and Crutzen, Paul J. "Atmospheric Change: An Earth System Perspective", W. H. Freeman & Co., New York, NY, USA, 1993, pp. 39-92.

3. Weitkamp, Claus "Lidar: Range-Resolved Optical Remote Sensing of the Atmosphere", Springer, New York, NY, USA, 2005, pp. 26-33.

4. Duck, Thomas "The Atmospheric-Optics Laboratory - Lidar Basics" Internet: http://aolab.phys.dal.ca/pages/LidarBasics, Sept. 2005.

5. De Young, Russell J.; Grant, William B.; and Severance, Kurt, "Aerosol Transport in the California Central Valley Observed by Airborne Lidar" *Environmental Science and Technology*, Vol. 39, pp. 8351-8357, 2005.

REPORT DOCUMENTATION PAGE

Form Approved
OMB No. 0704-0188

1. REPORT DATE *(DD-MM-YYYY)*	2. REPORT TYPE	3. DATES COVERED *(From - To)*
01- 01 - 2006	Technical Publication	October - December 2005

4. TITLE AND SUBTITLE

A Compact Efficient Lidar Receiver for Measuring Atmospheric Aerosols

5a. CONTRACT NUMBER

5b. GRANT NUMBER

5c. PROGRAM ELEMENT NUMBER

6. AUTHOR(S)

Gili, Christopher; and De Young, Russell

5d. PROJECT NUMBER

5e. TASK NUMBER

5f. WORK UNIT NUMBER

23-258-70-09

7. PERFORMING ORGANIZATION NAME(S) AND ADDRESS(ES)

NASA Langley Research Center
Hampton, VA 23681-2199

8. PERFORMING ORGANIZATION REPORT NUMBER

L-19206

9. SPONSORING/MONITORING AGENCY NAME(S) AND ADDRESS(ES)

National Aeronautics and Space Administration
Washington, DC 20546-0001

10. SPONSOR/MONITOR'S ACRONYM(S)

NASA

11. SPONSOR/MONITOR'S REPORT NUMBER(S)

NASA/TP-2006-213950

12. DISTRIBUTION/AVAILABILITY STATEMENT

Unclassified - Unlimited
Subject Category: 33 & 74
Availability: NASA CASI (301) 621-0390

13. SUPPLEMENTARY NOTES

Gili, Old Dominion University, Norfolk, VA
De Young, Langley Research Center, Hampton, VA
An electronic version can be found at http://ntrs.nasa.gov

14. ABSTRACT

A small, light weight, and efficient aerosol lidar receiver was constructed and tested. Weight and space savings were realized by using rigid optic tubes and mounting cubes to package the steering optics and detectors in a compact assembly. The receiver had a 1064nm channel using an APD detector. The 532nm channel was split (90/10) into an analog channel (90%) and a photon counting channel (10%). The efficiency of the 1064nm channel with optical filter was 44.0%. The efficiency of the analog 532nm channel was 61.4% with the optical filter, and the efficiency of the 532nm photon counting channel was 7.6% with the optical filter.

The results of the atmospheric tests show that the detectors were able to consistently return accurate results. The lidar receiver was able to detect distinct cloud layers, and the lidar returns also agreed across the different detectors. The use of a light weight fiber-coupled telescope reduced weight and allowed great latitude in detector assembly positioning due to the flexibility enabled by the use of fiber optics The receiver is now ready to be deployed for aircraft or ground based aerosol lidar measurements.

15. SUBJECT TERMS

Lidar Receiver; Aerosol Lidar; Optical Receiver

16. SECURITY CLASSIFICATION OF:			17. LIMITATION OF ABSTRACT	18. NUMBER OF PAGES	19a. NAME OF RESPONSIBLE PERSON
a. REPORT	b. ABSTRACT	c. THIS PAGE			STI Help Desk (email: help@sti.nasa.gov)
					19b. TELEPHONE NUMBER *(Include area code)*
U	U	U	UU	19	(301) 621-0390